Electromagnetic Scattering from a PEC Wedge Capped with Cylindrical Layers with Dielectric and Conductive Properties

Hulya OZTURK [1], *Korkut YEGIN* [2]

[1] Dept. of Mathematics, Gebze Technical University, Gebze, 41400 Kocaeli, Turkey
[2] Dept. of Electrical and Electronics Engineering, Ege University, Bornova, 35100 Izmir, Turkey

h.ozturk@gtu.edu.tr

Submitted June 15, 2016 / Accepted October 8, 2016

Abstract. *Electromagnetic scattering from a layered capped wedge is studied. The wedge is assumed infinite in z-direction (longitudinal) and capped with arbitrary layers of dielectric with varying thicknesses and dielectric properties including conductive loss. Scalar Helmholtz equation in two dimensions is formulated for each solution region and a matrix of unknown coefficients are arrived at for electric field representation. Closed form expressions are derived for 2- and 3-layer geometries. Numerical simulations are performed for different wedge shapes and dielectric layer properties and compared to PEC-only case. It has been shown that significant reduction in scattered electric field can be obtained with 2- and 3-layered cap geometries. Total electric field in the far field normalized to incident field is also computed as a precursor to RCS analysis. Analytical results can be useful in radar cross section analysis for aerial vehicles.*

Keywords

PEC wedge, dielectric capped wedge, electromagnetic wedge scattering, radar cross section

1. Introduction

Electromagnetic scattering from perfectly electrical conductor (PEC) wedge plays an important role in many applications ranging from radar cross section computation to antenna analysis. Especially, in airborne applications many parts of an airplane body can be represented by a wedge for radar cross section analysis. Since wedge angle can be varied to represent many structures, scattering from wedge is considered as a major canonical problem and has been extensively studied in the past [1–4]. Although many forms of wedge from dielectric covered [5], [6] to impedance boundary treated surfaces [7–10] have been reported, dielectric capped wedge for arbitrary layers of dielectric has not been studied. In this work, we present derivations for N-layer lossy dielectric capped wedge and closed form derivations for 2-layered and 3-layered dielectric capped wedge.

Scattering from PEC wedge due to infinite line source aligned with the longitudinal axis of the wedge is well known and scattering due to transverse magnetic (TM) plane wave excitation can be easily derived [3]. Although less studied, transverse electric (TE) case can also be derived using $\rho-$directed infinite line source. When the wedge is capped with a circular dielectric layer, analytical expressions for this case can be derived after some manipulations [5]. However, when more than one layer is assumed, the derivations get intricate and the effects of multilayer cap on resulting scattered field become less predictable. Especially if conductive losses in dielectric layers are assumed as in practical applications of such configuration, the effect of conductive loss may play a critical role in near- and far-field analysis. Thus, the contributions of present study are rigorous mathematical derivations for the general N-layer capped wedge problem with each layer having different electrical properties and analysis of electromagnetic scattering both in the near- and far-field of the structure, where near-field may represent antenna to antenna coupling and far-field for RCS computation.

Although the geometry of the problem assumes infinite direction on the wedge axis, its solution provides insightful information on electrically large finite objects. Despite scattering from electrically large finite structures can be computed using fast multipole methods (FMM) [11], [12] analytical closed form solutions for two dimensional problems such as the one stated here are still invaluable for researchers as they provide quick and reliable means for the scattered field.

We first present the system of equations for N-layer dielectric capped wedge where the dielectric layers are represented by simple constitutive parameters. In Sec. 3, we derive analytical expressions for 2-layered and 3-layered capped wedge. In Sec. 4, numerical results for 2-layer and 3-layer capped wedge with various thicknesses and constitutive parameters are obtained and compared to standalone

PEC wedge case for two different wedge angles, which are chosen to resemble airplane wing geometries. Conclusions are given in Sec. 5.

2. Arbitrarily Layered Dielectric Capped Wedge

A perfect electric conductor wedge which is capped with multiple (N-layers) dielectric cylinders, is presented in Fig. 1. The electric line current of amplitude I_e is assumed at (ρ_0, φ_0). Throughout the analysis, $e^{j\omega t}$ harmonic time dependence is assumed and suppressed. TM incident electric field is represented by

$$E_z^i = -I_e \frac{\omega\mu_0}{4} \mathrm{H}_0^{(2)} (k_0 \mid \rho - \rho_0 \mid) \tag{1}$$

where $\mathrm{H}_0^{(2)}(.)$ is the Hankel function of the second kind of order zero and $k_0 = \omega\sqrt{\varepsilon_0\mu_0}$. At wedge surfaces $\varphi = 0$ and $\varphi = 2\pi - \alpha$, $\mathbf{E}$ satisfies

$$\hat{\mathbf{n}} \times \mathbf{E} = 0 \tag{2}$$

where $\hat{\mathbf{n}}$ is the unit vector normal to the wedge surface. Taking into account the contribution on the φ dependence of (2), the z-components of the scattered electric field in their relevant regions can be determined as follows:

$$E_z^I (\rho, \varphi) = \sum_{n=1}^{\infty} a_{1n} \mathrm{J}_\nu (k_1\rho) \sin\nu\varphi \sin\nu\varphi_0,$$

$$E_z^m (\rho, \varphi) = \sum_{n=1}^{\infty} \left[a_{mn} \mathrm{J}_\nu (k_m\rho) \sin\nu\varphi \sin\nu\varphi_0 + b_{mn} \mathrm{H}_\nu^{(2)} (k_m\rho) \sin\nu\varphi \sin\nu\varphi_0\right], \quad m = 2, \ldots, N$$

$$E_z^{(N+1)} (\rho, \varphi) = \sum_{n=1}^{\infty} \left[a_{(N+1)n} \mathrm{J}_\nu (k_0\rho) \sin\nu\varphi \sin\nu\varphi_0 + b_{(N+1)n} \mathrm{H}_\nu^{(2)} (k_0\rho) \sin\nu\varphi \sin\nu\varphi_0\right],$$

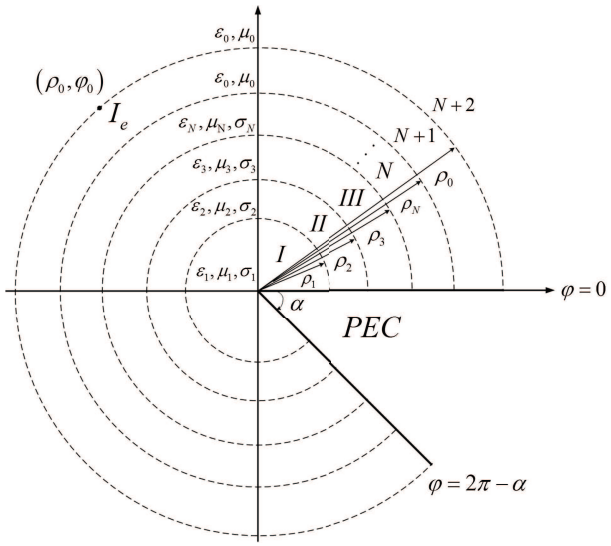

Fig. 1. The geometry of the problem.

$$E_z^{(N+2)} (\rho, \varphi) = \sum_{n=1}^{\infty} b_{(N+2)n} \mathrm{H}_\nu^{(2)} (k_0\rho) \sin\nu\varphi \sin\nu\varphi_0 \tag{3}$$

where $\mathrm{J}_\nu(.)$ is the ν^{th}-order Bessel function of the first kind, while $\mathrm{H}_\nu^{(2)}(.)$ is the ν^{th}-order Hankel function of the second kind, $k_m^2 = \omega^2\varepsilon_m\mu_m - j\omega\mu_m\sigma$ $(m = 2, \ldots, N)$ and $\nu = \frac{n\pi}{2\pi-\alpha}$. From Maxwell's equations, the field components can be expressed in terms of $E_z(\rho, \varphi)$ as

$$H_\varphi (\rho, \varphi) = \frac{1}{j\omega\mu} \frac{\partial E_z (\rho, \varphi)}{\partial\rho} \tag{4}$$

and

$$H_\rho (\rho, \varphi) = -\frac{1}{j\omega\mu} \frac{1}{\rho} \frac{\partial E_z (\rho, \varphi)}{\partial\varphi}. \tag{5}$$

Thus, the magnetic field components inside dielectric cylinders can be written as

$$\begin{aligned}
H_\varphi^I (\rho, \varphi) &= \frac{k_1}{j\omega\mu_1} \sum_{n=1}^{\infty} a_{1n} \mathrm{J}'_\nu (k_1\rho) \sin\nu\varphi \sin\nu\varphi_0, \\
H_\varphi^m (\rho, \varphi) &= \frac{k_m}{j\omega\mu_m} \sum_{n=1}^{\infty} \left[a_{mn} \mathrm{J}'_\nu (k_m\rho) \sin\nu\varphi \sin\nu\varphi_0 + b_{mn} \mathrm{H}'^{(2)}_\nu (k_m\rho) \sin\nu\varphi \sin\nu\varphi_0\right], \quad m = 2, \ldots, N \\
H_\varphi^{(N+1)} (\rho, \varphi) &= \frac{k_0}{j\omega\mu_0} \sum_{n=1}^{\infty} \left[a_{(N+1)n} \mathrm{J}'_\nu (k_0\rho) \sin\nu\varphi \sin\nu\varphi_0 + b_{(N+1)n} \mathrm{H}'^{(2)}_\nu (k_0\rho) \sin\nu\varphi \sin\nu\varphi_0\right], \\
H_\varphi^{(N+2)} (\rho, \varphi) &= \frac{k_0}{j\omega\mu_0} \sum_{n=1}^{\infty} b_{(N+2)n} \mathrm{H}'^{(2)}_\nu (k_0\rho) \sin\nu\varphi \sin\nu\varphi_0
\end{aligned} \tag{6}$$

and

$$H_\rho^I (\rho, \varphi) = -\frac{1}{j\omega\mu_1\rho} \sum_{n=1}^{\infty} a_{1n} \mathrm{J}_\nu (k_1\rho)\, \nu \cos\nu\varphi \sin\nu\varphi_0,$$

$$H_\rho^m(\rho,\varphi) = -\frac{1}{\mathrm{j}\omega\mu_m\rho}\sum_{n=1}^{\infty}\left[a_{mn}\mathrm{J}_\nu(k_m\rho)\,\nu\cos\nu\varphi\sin\nu\varphi_0 + b_{mn}\mathrm{H}_\nu^{(2)}(k_m\rho)\,\nu\cos\nu\varphi\sin\nu\varphi_0\right],\quad m=2,\ldots,N$$
$$H_\rho^{(N+1)}(\rho,\varphi) = -\frac{1}{\mathrm{j}\omega\mu_0\rho}\sum_{n=1}^{\infty}\left[a_{(N+1)n}\mathrm{J}_\nu(k_0\rho)\,\nu\cos\nu\varphi\sin\nu\varphi_0 + b_{(N+1)n}\mathrm{H}_\nu^{(2)}(k_0\rho)\,\nu\cos\nu\varphi\sin\nu\varphi_0\right], \tag{7}$$
$$H_\rho^{(N+2)}(\rho,\varphi) = -\frac{1}{\mathrm{j}\omega\mu_0\rho}\sum_{n=1}^{\infty}b_{(N+2)n}\mathrm{H}_\nu^{(2)}(k_0\rho)\,\nu\cos\nu\varphi\sin\nu\varphi_0.$$

In (6), prime denotes the first-degree derivative with respect to ρ. The unknown coefficients a_{mn} and b_{mn} $(m = 1,\ldots,N+2)$ can be determined with the help of the following continuity conditions at $\rho = \rho_m$ $(m = 1,\ldots,N)$:

$$\begin{cases} E_z^m(\rho_m,\varphi) = E_z^{m+1}(\rho_m,\varphi) \\ H_\varphi^m(\rho_m,\varphi) = H_\varphi^{m+1}(\rho_m,\varphi) \end{cases},\quad m=1,\ldots,N \tag{8}$$

$$\begin{cases} E_z^{(N+1)}(\rho_0,\varphi) = E_z^{(N+2)}(\rho_0,\varphi) \\ H_\varphi^{(N+1)}(\rho_0,\varphi) = H_\varphi^{(N+2)}(\rho_0,\varphi) + J_e \end{cases}, \tag{9}$$

where J_e denotes the current density. J_e can be expressed as

$$J_e = \frac{I_e}{\rho_0}\frac{2}{2\pi-\alpha}\sum_{n=1}^{\infty}\sin\nu\varphi\sin\nu\varphi_0, \tag{10}$$

Application of (8) and (9) at $\rho = \rho_m$ $(m = 1,\ldots,N)$ yields:

$$a_{1n}\mathrm{J}_\nu(k_1\rho_1) - a_{2n}\mathrm{J}_\nu(k_2\rho_1) - b_{2n}\mathrm{H}_\nu^{(2)}(k_2\rho_1) = 0, \tag{11}$$
$$\frac{k_1}{\mu_1}a_{1n}\mathrm{J}_\nu'(k_1\rho_1) - \frac{k_2}{\mu_2}\left\{a_{2n}\mathrm{J}_\nu'(k_2\rho_1) + b_{2n}\mathrm{H}_\nu'^{(2)}(k_2\rho_1)\right\} = 0, \tag{12}$$

$$a_{mn}\mathrm{J}_\nu(k_m\rho_m) - a_{(m+1)n}\mathrm{J}_\nu(k_{(m+1)}\rho_m) + b_{mn}\mathrm{H}_\nu^{(2)}(k_m\rho_m) - b_{(m+1)n}\mathrm{H}_\nu^{(2)}(k_{(m+1)}\rho_m) = 0,\quad m=2,\ldots,N-1 \tag{13}$$

$$\frac{k_m}{\mu_m}\left\{a_{mn}\mathrm{J}_\nu'(k_m\rho_m) + b_{mn}\mathrm{H}_\nu'^{(2)}(k_m\rho_m)\right\} - \frac{k_{(m+1)}}{\mu_{(m+1)}}\left\{a_{(m+1)n}\mathrm{J}_\nu'(k_{(m+1)}\rho_m) + b_{(m+1)n}\mathrm{H}_\nu'^{(2)}(k_{(m+1)}\rho_m)\right\} = 0,\quad m=2,\ldots,N-1 \tag{14}$$

$$a_{Nn}\mathrm{J}_\nu(k_N\rho_N) - a_{(N+1)n}\mathrm{J}_\nu(k_0\rho_N) + b_{Nn}\mathrm{H}_\nu^{(2)}(k_N\rho_N) - b_{(N+1)n}\mathrm{H}_\nu^{(2)}(k_0\rho_N) = 0, \tag{15}$$

$$\frac{k_N}{\mu_N}\left\{a_{Nn}\mathrm{J}_\nu'(k_N\rho_N) + b_{Nn}\mathrm{H}_\nu'^{(2)}(k_N\rho_N)\right\} - \frac{k_0}{\mu_0}\left\{a_{(N+1)n}\mathrm{J}_\nu'(k_0\rho_N) + b_{(N+1)n}\mathrm{H}_\nu'^{(2)}(k_0\rho_N)\right\} = 0, \tag{16}$$

$$a_{(N+1)n}\mathrm{J}_\nu(k_0\rho_0) + b_{(N+1)n}\mathrm{H}_\nu^{(2)}(k_0\rho_0) - b_{(N+2)n}\mathrm{H}_\nu^{(2)}(k_0\rho_0) = 0, \tag{17}$$

$$a_{(N+1)n}\mathrm{J}_\nu'(k_0\rho_0) + b_{(N+1)n}\mathrm{H}_\nu'^{(2)}(k_0\rho_0) - b_{(N+2)n}\mathrm{H}_\nu'^{(2)}(k_0\rho_0) = -\frac{I_e}{\rho_0}\frac{2}{2\pi-\alpha}\frac{\mathrm{j}\omega\mu_0}{k_0}. \tag{18}$$

These (2N+2) x(2N+2) system of algebraic equations can be solved numerically and the expansion coefficients a_{mn} and b_{mn} $(m = 1,\ldots,N+2)$ can be fully determined.

3. 2-Layer and 3-Layer Capped Wedge

Explicit forms of the unknown coefficients for $N = 2$ and $N = 3$ can be derived as follows. For $N = 2$ case,

$$a_{1n} = \frac{k_2\left\{\mathrm{H}_\nu^{(2)}(k_0\rho_2)\,\mathrm{J}_\nu'(k_0\rho_2) - \mathrm{H}_\nu'^{(2)}(k_0\rho_2)\,\mathrm{J}_\nu(k_0\rho_2)\right\}}{\mu_2 D(k_0,k_1,k_2,\rho_0,\rho_1,\rho_2)}\left\{\mathrm{H}_\nu^{(2)}(k_2\rho_1)\,\mathrm{J}_\nu'(k_2\rho_1) - \mathrm{H}_\nu'^{(2)}(k_2\rho_1)\,\mathrm{J}_\nu(k_2\rho_1)\right\}, \tag{19}$$

$$a_{2n} = \frac{\left\{\frac{k_1}{\mu_1}\mathrm{H}_\nu^{(2)}(k_2\rho_1)\,\mathrm{J}_\nu'(k_1\rho_1) - \frac{k_2}{\mu_2}\mathrm{H}_\nu'^{(2)}(k_2\rho_1)\,\mathrm{J}_\nu(k_1\rho_1)\right\}}{D(k_0,k_1,k_2,\rho_0,\rho_1,\rho_2)}\left\{\mathrm{H}_\nu^{(2)}(k_0\rho_2)\,\mathrm{J}_\nu'(k_0\rho_2) - \mathrm{H}_\nu'^{(2)}(k_0\rho_2)\,\mathrm{J}_\nu(k_0\rho_2)\right\}, \tag{20}$$

$$a_{3n} = \frac{\mu_0}{k_0 D(k_0,k_1,k_2,\rho_0,\rho_1,\rho_2)}\left[\left\{\frac{k_2}{\mu_2}\mathrm{H}_\nu'^{(2)}(k_2\rho_1)\,\mathrm{J}_\nu(k_1\rho_1) - \frac{k_1}{\mu_1}\mathrm{H}_\nu^{(2)}(k_2\rho_1)\,\mathrm{J}_\nu'(k_1\rho_1)\right\}\left\{\frac{k_0}{\mu_0}\mathrm{H}_\nu'^{(2)}(k_0\rho_2)\,\mathrm{J}_\nu(k_2\rho_2) - \frac{k_2}{\mu_2}\mathrm{H}_\nu^{(2)}(k_0\rho_2)\,\mathrm{J}_\nu'(k_2\rho_2)\right\} + \left\{\frac{k_2}{\mu_2}\mathrm{H}_\nu^{(2)}(k_0\rho_2)\,\mathrm{H}_\nu'^{(2)}(k_2\rho_2) - \frac{k_0}{\mu_0}\mathrm{H}_\nu'^{(2)}(k_0\rho_2)\,\mathrm{H}_\nu^{(2)}(k_2\rho_2)\right\}\left\{\frac{k_2}{\mu_2}\mathrm{J}_\nu'(k_2\rho_1)\,\mathrm{J}_\nu(k_1\rho_1) - \frac{k_1}{\mu_1}\mathrm{J}_\nu'(k_1\rho_1)\,\mathrm{J}_\nu(k_2\rho_1)\right\}\right], \tag{21}$$

$$b_{2n} = \frac{\left\{\mathrm{H}_\nu^{(2)}(k_0\rho_2)\,\mathrm{J}'_\nu(k_0\rho_2) - \mathrm{H}'^{(2)}_\nu(k_0\rho_2)\,\mathrm{J}_\nu(k_0\rho_2)\right\}}{D(k_0,k_1,k_2,\rho_0,\rho_1,\rho_2)} \left\{\frac{k_2}{\mu_2}\mathrm{J}'_\nu(k_2\rho_1)\,\mathrm{J}_\nu(k_1\rho_1) - \frac{k_1}{\mu_1}\mathrm{J}'_\nu(k_1\rho_1)\,\mathrm{J}_\nu(k_2\rho_1)\right\}, \quad (22)$$

$$b_{3n} = \frac{\mu_0}{k_0}\frac{1}{D(k_0,k_1,k_2,\rho_0,\rho_1,\rho_2)} \left[\left\{\frac{k_2}{\mu_2}\mathrm{H}'^{(2)}_\nu(k_2\rho_1)\,\mathrm{J}_\nu(k_1\rho_1) - \frac{k_1}{\mu_1}\mathrm{H}_\nu^{(2)}(k_2\rho_1)\,\mathrm{J}'_\nu(k_1\rho_1)\right\}\left\{\frac{k_2}{\mu_2}\mathrm{J}_\nu(k_0\rho_2)\,\mathrm{J}'_\nu(k_2\rho_2) - \frac{k_0}{\mu_0}\mathrm{J}_\nu(k_2\rho_2)\,\mathrm{J}'_\nu(k_0\rho_2)\right\} + \left\{\frac{k_2}{\mu_2}\mathrm{J}_\nu(k_1\rho_1)\,\mathrm{J}'_\nu(k_2\rho_1) - \frac{k_1}{\mu_1}\mathrm{J}'_\nu(k_1\rho_1)\,\mathrm{J}_\nu(k_2\rho_1)\right\}\left\{\frac{k_0}{\mu_0}\mathrm{H}_\nu^{(2)}(k_2\rho_2)\,\mathrm{J}'_\nu(k_0\rho_2) - \frac{k_2}{\mu_2}\mathrm{H}'^{(2)}_\nu(k_2\rho_2)\,\mathrm{J}_\nu(k_0\rho_2)\right\}\right], \quad (23)$$

$$b_{4n} = -b_{3n} + \frac{\mu_0}{k_0\mathrm{H}_\nu^{(2)}(k_0\rho_0)}\frac{\mathrm{J}_\nu(k_0\rho_0)}{D(k_0,k_1,k_2,\rho_0,\rho_1,\rho_2)} \left[\left\{\frac{k_2}{\mu_2}\mathrm{H}'^{(2)}_\nu(k_2\rho_1)\,\mathrm{J}_\nu(k_1\rho_1) - \frac{k_1}{\mu_1}\mathrm{H}_\nu^{(2)}(k_2\rho_1)\,\mathrm{J}'_\nu(k_1\rho_1)\right\}\left\{\frac{k_0}{\mu_0}\mathrm{J}_\nu(k_2\rho_2)\,\mathrm{H}'^{(2)}_\nu(k_0\rho_2) - \frac{k_2}{\mu_2}\mathrm{J}'_\nu(k_2\rho_2)\,\mathrm{H}_\nu^{(2)}(k_0\rho_2)\right\} + \left\{\frac{k_2}{\mu_2}\mathrm{J}'_\nu(k_2\rho_1)\,\mathrm{J}_\nu(k_1\rho_1) - \frac{k_1}{\mu_1}\mathrm{J}'_\nu(k_1\rho_1)\,\mathrm{J}_\nu(k_2\rho_1)\right\}\left\{\frac{k_2}{\mu_2}\mathrm{H}_\nu^{(2)}(k_0\rho_2)\,\mathrm{H}'^{(2)}_\nu(k_2\rho_2) - \frac{k_0}{\mu_0}\mathrm{H}'^{(2)}_\nu(k_0\rho_2)\,\mathrm{H}_\nu^{(2)}(k_2\rho_2)\right\}\right] \quad (24)$$

with

$$D(k_0,k_1,k_2,\rho_0,\rho_1,\rho_2) = \frac{\rho_0(2\pi-\alpha)}{2I_e\mathrm{j}\omega\mathrm{H}_\nu^{(2)}(k_0\rho_0)}\left\{\mathrm{H}_\nu^{(2)}(k_0\rho_0)\,\mathrm{J}'_\nu(k_0\rho_0) - \mathrm{H}'^{(2)}_\nu(k_0\rho_0)\,\mathrm{J}_\nu(k_0\rho_0)\right\} \left[\left\{\frac{k_2}{\mu_2}\mathrm{J}'_\nu(k_2\rho_1)\,\mathrm{J}_\nu(k_1\rho_1) - \frac{k_1}{\mu_1}\mathrm{J}'_\nu(k_1\rho_1)\,\mathrm{J}_\nu(k_2\rho_1)\right\}\left\{\frac{k_0}{\mu_0}\mathrm{H}'^{(2)}_\nu(k_0\rho_2)\,\mathrm{H}_\nu^{(2)}(k_2\rho_2) - \frac{k_2}{\mu_2}\mathrm{H}'^{(2)}_\nu(k_2\rho_2)\,\mathrm{H}_\nu^{(2)}(k_0\rho_2)\right\} - \left\{\frac{k_2}{\mu_2}\mathrm{H}'^{(2)}_\nu(k_2\rho_1)\,\mathrm{J}_\nu(k_1\rho_1) - \frac{k_1}{\mu_1}\mathrm{J}'_\nu(k_1\rho_1)\,\mathrm{H}_\nu^{(2)}(k_2\rho_1)\right\}\left\{\frac{k_0}{\mu_0}\mathrm{H}'^{(2)}_\nu(k_0\rho_2)\,\mathrm{J}_\nu(k_2\rho_2) - \frac{k_2}{\mu_2}\mathrm{H}_\nu^{(2)}(k_0\rho_2)\,\mathrm{J}'_\nu(k_2\rho_2)\right\}\right]. \quad (25)$$

The plane wave excitation ($\rho_0 \to \infty$) can be computed using the asymptotic expansion of $\mathrm{H}_\nu^{(2)}(k_0\rho_0)$ for large argument as

$$\mathrm{H}_\nu^{(2)}(k_0\rho_0) \simeq \sqrt{\frac{2}{\pi k_0\rho_0}}\mathrm{e}^{-\mathrm{j}\left(k_0\rho_0 - \frac{\nu\pi}{2} - \frac{\pi}{4}\right)}. \quad (26)$$

In this case, the unknown coefficients become

$$a_{1n} = -\frac{k_0k_2\left\{\mathrm{H}_\nu^{(2)}(k_0\rho_2)\,\mathrm{J}'_\nu(k_0\rho_2) - \mathrm{H}'^{(2)}_\nu(k_0\rho_2)\,\mathrm{J}_\nu(k_0\rho_2)\right\}}{\mu_0\mu_2\tilde{D}(k_0,k_1,k_2,\rho_1,\rho_2)}\left\{\mathrm{H}_\nu^{(2)}(k_2\rho_1)\,\mathrm{J}'_\nu(k_2\rho_1) - \mathrm{H}'^{(2)}_\nu(k_2\rho_1)\,\mathrm{J}_\nu(k_2\rho_1)\right\}, \quad (27)$$

$$a_{2n} = \frac{k_0\left\{\mathrm{H}_\nu^{(2)}(k_0\rho_2)\,\mathrm{J}'_\nu(k_0\rho_2) - \mathrm{H}'^{(2)}_\nu(k_0\rho_2)\,\mathrm{J}_\nu(k_0\rho_2)\right\}}{\mu_0\tilde{D}(k_0,k_1,k_2,\rho_1,\rho_2)}\left\{\frac{k_1}{\mu_1}\mathrm{H}_\nu^{(2)}(k_2\rho_1)\,\mathrm{J}'_\nu(k_1\rho_1) - \frac{k_2}{\mu_2}\mathrm{H}'^{(2)}_\nu(k_2\rho_1)\,\mathrm{J}_\nu(k_1\rho_1)\right\}, \quad (28)$$

$$a_{3n} = \frac{1}{\tilde{D}(k_0,k_1,k_2,\rho_1,\rho_2)} \left[\left\{\frac{k_2}{\mu_2}\mathrm{H}'^{(2)}_\nu(k_2\rho_1)\,\mathrm{J}_\nu(k_1\rho_1) - \frac{k_1}{\mu_1}\mathrm{H}_\nu^{(2)}(k_2\rho_1)\,\mathrm{J}'_\nu(k_1\rho_1)\right\}\left\{\frac{k_0}{\mu_0}\mathrm{H}'^{(2)}_\nu(k_0\rho_2)\,\mathrm{J}_\nu(k_2\rho_2) - \frac{k_2}{\mu_2}\mathrm{H}_\nu^{(2)}(k_0\rho_2)\,\mathrm{J}'_\nu(k_2\rho_2)\right\} + \left\{\frac{k_2}{\mu_2}\mathrm{H}_\nu^{(2)}(k_0\rho_2)\,\mathrm{H}'^{(2)}_\nu(k_2\rho_2) - \frac{k_0}{\mu_0}\mathrm{H}'^{(2)}_\nu(k_0\rho_2)\,\mathrm{H}_\nu^{(2)}(k_2\rho_2)\right\}\left\{\frac{k_2}{\mu_2}\mathrm{J}'_\nu(k_2\rho_1)\,\mathrm{J}_\nu(k_1\rho_1) - \frac{k_1}{\mu_1}\mathrm{J}'_\nu(k_1\rho_1)\,\mathrm{J}_\nu(k_2\rho_1)\right\}\right], \quad (29)$$

$$b_{2n} = \frac{\mathrm{j}\omega \left\{ \mathrm{H}_{\nu}^{(2)}(k_0\rho_2)\,\mathrm{J}'_{\nu}(k_0\rho_2) - \mathrm{H}'^{(2)}_{\nu}(k_0\rho_2)\,\mathrm{J}_{\nu}(k_0\rho_2) \right\}}{\tilde{D}(k_0, k_1, k_2, \rho_1, \rho_2)} \left\{ \frac{k_2}{\mu_2}\mathrm{J}'_{\nu}(k_2\rho_1)\,\mathrm{J}_{\nu}(k_1\rho_1) - \frac{k_1}{\mu_1}\mathrm{J}'_{\nu}(k_1\rho_1)\,\mathrm{J}_{\nu}(k_2\rho_1) \right\}, \tag{30}$$

$$\begin{aligned} b_{3n} = {} & \frac{1}{\tilde{D}(k_0, k_1, k_2, \rho_1, \rho_2)} \\ & \left[\left\{ \frac{k_2}{\mu_2}\mathrm{H}'^{(2)}_{\nu}(k_2\rho_1)\,\mathrm{J}_{\nu}(k_1\rho_1) - \frac{k_1}{\mu_1}\mathrm{H}^{(2)}_{\nu}(k_2\rho_1)\,\mathrm{J}'_{\nu}(k_1\rho_1) \right\} \left\{ \frac{k_2}{\mu_2}\mathrm{J}_{\nu}(k_0\rho_2)\,\mathrm{J}'_{\nu}(k_2\rho_2) - \frac{k_0}{\mu_0}\mathrm{J}_{\nu}(k_2\rho_2)\,\mathrm{J}'_{\nu}(k_0\rho_2) \right\} + \right. \\ & \left. \left\{ \frac{k_2}{\mu_2}\mathrm{J}_{\nu}(k_1\rho_1)\,\mathrm{J}'_{\nu}(k_2\rho_1) - \frac{k_1}{\mu_1}\mathrm{J}'_{\nu}(k_1\rho_1)\,\mathrm{J}_{\nu}(k_2\rho_1) \right\} \left\{ \frac{k_0}{\mu_0}\mathrm{H}^{(2)}_{\nu}(k_2\rho_2)\,\mathrm{J}'_{\nu}(k_0\rho_2) - \frac{k_2}{\mu_2}\mathrm{H}'^{(2)}_{\nu}(k_2\rho_2)\,\mathrm{J}_{\nu}(k_0\rho_2) \right\} \right] \end{aligned} \tag{31}$$

where

$$\begin{aligned} \tilde{D}(k_0, k_1, k_2, \rho_1, \rho_2) = {} & -\frac{2\pi - \alpha}{4\mathrm{j}^{\nu}\pi} \\ & \left\{ \frac{k_2}{\mu_2}\mathrm{J}'_{\nu}(k_2\rho_1)\,\mathrm{J}_{\nu}(k_1\rho_1) - \frac{k_1}{\mu_1}\mathrm{J}'_{\nu}(k_1\rho_1)\,\mathrm{J}_{\nu}(k_2\rho_1) \right\} \left\{ \frac{k_0}{\mu_0}\mathrm{H}'^{(2)}_{\nu}(k_0\rho_2)\,\mathrm{H}^{(2)}_{\nu}(k_2\rho_2) - \frac{k_2}{\mu_2}\mathrm{H}'^{(2)}_{\nu}(k_2\rho_2)\,\mathrm{H}^{(2)}_{\nu}(k_0\rho_2) \right\} + \\ & \left\{ \frac{k_2}{\mu_2}\mathrm{H}'^{(2)}_{\nu}(k_2\rho_1)\,\mathrm{J}_{\nu}(k_1\rho_1) - \frac{k_1}{\mu_1}\mathrm{J}'_{\nu}(k_1\rho_1)\,\mathrm{H}^{(2)}_{\nu}(k_2\rho_1) \right\} \left\{ \frac{k_2}{\mu_2}\mathrm{H}^{(2)}_{\nu}(k_0\rho_2)\,\mathrm{J}'_{\nu}(k_2\rho_2) - \frac{k_0}{\mu_0}\mathrm{H}'^{(2)}_{\nu}(k_0\rho_2)\,\mathrm{J}_{\nu}(k_2\rho_2) \right\}. \end{aligned} \tag{32}$$

In (27)–(32), all the coefficients are normalized with incident plane wave which is given by

$$E_0 = -I_e \frac{\omega\mu_0}{4}\sqrt{\frac{2j}{\pi k_0\rho_0}}\mathrm{e}^{-\mathrm{j}k_0\rho_0}. \tag{33}$$

For $N = 3$ case

$$\begin{aligned} a_{1n} = {} & \left[\frac{k_2k_3 \left\{ \mathrm{H}_{\nu}^{(2)}(k_0\rho_3)\,\mathrm{J}'_{\nu}(k_0\rho_3) - \mathrm{H}'^{(2)}_{\nu}(k_0\rho_3)\,\mathrm{J}_{\nu}(k_0\rho_3) \right\}}{\mu_2\mu_3 R(k_0, k_1, k_2, k_3, \rho_0, \rho_1, \rho_2, \rho_3)} \right] \\ & \left[\left\{ \mathrm{H}_{\nu}^{(2)}(k_3\rho_2)\,\mathrm{J}'_{\nu}(k_3\rho_2) - \mathrm{H}'^{(2)}_{\nu}(k_3\rho_2)\,\mathrm{J}_{\nu}(k_3\rho_2) \right\} \left\{ \mathrm{H}'^{(2)}_{\nu}(k_2\rho_1)\,\mathrm{J}_{\nu}(k_2\rho_1) - \mathrm{H}^{(2)}_{\nu}(k_2\rho_1)\,\mathrm{J}'_{\nu}(k_2\rho_1) \right\} \right], \end{aligned} \tag{34}$$

$$\begin{aligned} a_{2n} = {} & \left[\frac{k_3 \left\{ \frac{k_1}{\mu_1}\mathrm{H}_{\nu}^{(2)}(k_2\rho_1)\,\mathrm{J}'_{\nu}(k_1\rho_1) - \frac{k_2}{\mu_2}\mathrm{H}'^{(2)}_{\nu}(k_2\rho_1)\,\mathrm{J}_{\nu}(k_1\rho_1) \right\}}{\mu_3 R(k_0, k_1, k_2, k_3, \rho_0, \rho_1, \rho_2, \rho_3)} \right] \\ & \left[\left\{ \mathrm{H}_{\nu}^{(2)}(k_3\rho_2)\,\mathrm{J}'_{\nu}(k_3\rho_2) - \mathrm{H}'^{(2)}_{\nu}(k_3\rho_2)\,\mathrm{J}_{\nu}(k_3\rho_2) \right\} \left\{ \mathrm{H}'^{(2)}_{\nu}(k_0\rho_3)\,\mathrm{J}_{\nu}(k_0\rho_3) - \mathrm{H}^{(2)}_{\nu}(k_0\rho_3)\,\mathrm{J}'_{\nu}(k_0\rho_3) \right\} \right], \end{aligned} \tag{35}$$

$$a_{3n} = A(k_1, k_2, k_3, \rho_1, \rho_2, \rho_3) \frac{\left\{ \mathrm{H}_{\nu}^{(2)}(k_0\rho_3)\,\mathrm{J}'_{\nu}(k_0\rho_3) - \mathrm{H}'^{(2)}_{\nu}(k_0\rho_3)\,\mathrm{J}_{\nu}(k_0\rho_3) \right\}}{R(k_0, k_1, k_2, k_3, \rho_0, \rho_1, \rho_2, \rho_3)}, \tag{36}$$

$$\begin{aligned} a_{4n} = {} & \frac{\mu_0}{k_0} \frac{1}{R(k_0, k_1, k_2, k_3, \rho_0, \rho_1, \rho_2, \rho_3)} \\ & \left[\frac{k_3}{\mu_3}\mathrm{H}_{\nu}^{(2)}(k_0\rho_3) \left\{ \mathrm{J}'_{\nu}(k_3\rho_3)\,A(k_1, k_2, k_3, \rho_1, \rho_2, \rho_3) + \mathrm{H}'^{(2)}_{\nu}(k_3\rho_3)\,B(k_1, k_2, k_3, \rho_1, \rho_2, \rho_3) \right\} - \right. \\ & \left. \frac{k_0}{\mu_0}\mathrm{H}'^{(2)}_{\nu}(k_0\rho_3) \left\{ \mathrm{J}_{\nu}(k_3\rho_3)\,A(k_1, k_2, k_3, \rho_1, \rho_2, \rho_3) + \mathrm{H}^{(2)}_{\nu}(k_3\rho_3)\,B(k_1, k_2, k_3, \rho_1, \rho_2, \rho_3) \right\} \right], \end{aligned} \tag{37}$$

$$b_{2n} = \frac{k_3 \left\{ \mathrm{H}_\nu^{(2)}(k_0\rho_3)\,\mathrm{J}'_\nu(k_0\rho_3) - \mathrm{H}'^{(2)}_\nu(k_0\rho_3)\,\mathrm{J}_\nu(k_0\rho_3) \right\}}{\mu_3 R(k_0, k_1, k_2, k_3, \rho_0, \rho_1, \rho_2, \rho_3)}$$
$$\left[\left\{ \mathrm{H}_\nu^{(2)}(k_3\rho_2)\,\mathrm{J}'_\nu(k_3\rho_2) - \mathrm{H}'^{(2)}_\nu(k_3\rho_2)\,\mathrm{J}_\nu(k_3\rho_2) \right\} \left\{ \frac{k_2}{\mu_2}\mathrm{J}'_\nu(k_2\rho_1)\,\mathrm{J}_\nu(k_1\rho_1) - \frac{k_1}{\mu_1}\mathrm{J}'_\nu(k_1\rho_1)\,\mathrm{J}_\nu(k_2\rho_1) \right\} \right], \quad (38)$$

$$b_{3n} = B(k_1, k_2, k_3, \rho_1, \rho_2, \rho_3)\, \frac{\left\{ \mathrm{H}_\nu^{(2)}(k_0\rho_3)\,\mathrm{J}'_\nu(k_0\rho_3) - \mathrm{H}'^{(2)}_\nu(k_0\rho_3)\,\mathrm{J}_\nu(k_0\rho_3) \right\}}{R(k_0, k_1, k_2, k_3, \rho_0, \rho_1, \rho_2, \rho_3)}, \quad (39)$$

$$b_{4n} = \frac{\mu_0}{k_0} \frac{1}{R(k_0, k_1, k_2, k_3, \rho_0, \rho_1, \rho_2, \rho_3)}$$
$$\left[\frac{k_3}{\mu_3}\mathrm{J}_\nu(k_0\rho_3) \left\{ \mathrm{J}'_\nu(k_3\rho_3)\, A(k_1, k_2, k_3, \rho_1, \rho_2, \rho_3) + \mathrm{H}'^{(2)}_\nu(k_3\rho_3)\, B(k_1, k_2, k_3, \rho_1, \rho_2, \rho_3) \right\} - \right.$$
$$\left. \frac{k_0}{\mu_0}\mathrm{J}'_\nu(k_0\rho_3) \left\{ \mathrm{J}_\nu(k_3\rho_3)\, A(k_1, k_2, k_3, \rho_1, \rho_2, \rho_3) + \mathrm{H}^{(2)}_\nu(k_3\rho_3)\, B(k_1, k_2, k_3, \rho_1, \rho_2, \rho_3) \right\} \right], \quad (40)$$

$$b_{5n} = -b_{4n} + \frac{\mu_0 \mathrm{J}_\nu(k_0\rho_0)}{k_0 \mathrm{H}_\nu^{(2)}(k_0\rho_0)\, R(k_0, k_1, k_2, k_3, \rho_0, \rho_1, \rho_2, \rho_3)}$$
$$\left[\frac{k_3}{\mu_3}\mathrm{H}_\nu^{(2)}(k_0\rho_3) \left\{ \mathrm{J}'_\nu(k_3\rho_3)\, A(k_1, k_2, k_3, \rho_1, \rho_2, \rho_3) + \mathrm{H}'^{(2)}_\nu(k_3\rho_3)\, B(k_1, k_2, k_3, \rho_1, \rho_2, \rho_3) \right\} - \right.$$
$$\left. \frac{k_0}{\mu_0}\mathrm{H}'^{(2)}_\nu(k_0\rho_3) \left\{ \mathrm{J}_\nu(k_3\rho_3)\, A(k_1, k_2, k_3, \rho_1, \rho_2, \rho_3) + \mathrm{H}^{(2)}_\nu(k_3\rho_3)\, B(k_1, k_2, k_3, \rho_1, \rho_2, \rho_3) \right\} \right] \quad (41)$$

where

$$R(k_0, k_1, k_2, k_3, \rho_0, \rho_1, \rho_2, \rho_3) =$$
$$\frac{\rho_0(2\pi - \alpha)}{2I_e \mathrm{j}\omega \mathrm{H}_\nu^{(2)}(k_0\rho_0)} \left[\mathrm{H}'^{(2)}_\nu(k_0\rho_0)\,\mathrm{J}_\nu(k_0\rho_0) - \mathrm{H}^{(2)}_\nu(k_0\rho_0)\,\mathrm{J}'_\nu(k_0\rho_0) \right]$$
$$\left[\left[\frac{k_0 k_3}{\mu_0\mu_3}\mathrm{H}'^{(2)}_\nu(k_0\rho_3) \left\{ \mathrm{H}^{(2)}_\nu(k_3\rho_3)\,\mathrm{J}'_\nu(k_3\rho_2) - \mathrm{H}'^{(2)}_\nu(k_3\rho_2)\,\mathrm{J}_\nu(k_3\rho_3) \right\} + \right. \right.$$
$$\left. \frac{k_3^2}{\mu_3^2}\mathrm{H}^{(2)}_\nu(k_0\rho_3) \left\{ \mathrm{H}'^{(2)}_\nu(k_3\rho_2)\,\mathrm{J}'_\nu(k_3\rho_3) - \mathrm{H}'^{(2)}_\nu(k_3\rho_3)\,\mathrm{J}'_\nu(k_3\rho_2) \right\} \right]$$
$$\left[\frac{k_2}{\mu_2}\mathrm{J}_\nu(k_1\rho_1) \left\{ \mathrm{H}^{(2)}_\nu(k_2\rho_2)\,\mathrm{J}'_\nu(k_2\rho_1) - \mathrm{H}'^{(2)}_\nu(k_2\rho_1)\,\mathrm{J}_\nu(k_3\rho_2) \right\} + \right.$$
$$\left. \frac{k_1}{\mu_1}\mathrm{J}'_\nu(k_1\rho_1) \left\{ \mathrm{H}^{(2)}_\nu(k_2\rho_1)\,\mathrm{J}_\nu(k_2\rho_2) - \mathrm{H}^{(2)}_\nu(k_2\rho_2)\,\mathrm{J}_\nu(k_2\rho_1) \right\} \right] +$$
$$\left[\frac{k_3}{\mu_3}\mathrm{H}^{(2)}_\nu(k_0\rho_3) \left\{ \mathrm{H}^{(2)}_\nu(k_3\rho_2)\,\mathrm{J}'_\nu(k_3\rho_3) - \mathrm{H}'^{(2)}_\nu(k_3\rho_3)\,\mathrm{J}_\nu(k_3\rho_2) \right\} + \right.$$
$$\left. \frac{k_0}{\mu_0}\mathrm{H}'^{(2)}_\nu(k_0\rho_3) \left\{ \mathrm{H}^{(2)}_\nu(k_3\rho_3)\,\mathrm{J}_\nu(k_3\rho_2) - \mathrm{H}^{(2)}_\nu(k_3\rho_2)\,\mathrm{J}_\nu(k_3\rho_3) \right\} \right]$$
$$\left[\frac{k_2^2}{\mu_2^2}\mathrm{J}_\nu(k_1\rho_1) \left\{ \mathrm{H}'^{(2)}_\nu(k_2\rho_1)\,\mathrm{J}'_\nu(k_2\rho_2) - \mathrm{H}'^{(2)}_\nu(k_2\rho_2)\,\mathrm{J}'_\nu(k_2\rho_1) \right\} + \right.$$
$$\left. \left. \frac{k_1 k_2}{\mu_1\mu_2}\mathrm{J}'_\nu(k_1\rho_1) \left\{ \mathrm{H}'^{(2)}_\nu(k_2\rho_2)\,\mathrm{J}_\nu(k_2\rho_1) - \mathrm{H}^{(2)}_\nu(k_2\rho_1)\,\mathrm{J}'_\nu(k_2\rho_2) \right\} \right] \right], \quad (42)$$

and

$$A(k_1,k_2,k_3,\rho_1,\rho_2,\rho_3) = \left[\frac{k_2^2}{\mu_2^2}\mathrm{H}_\nu^{(2)}(k_3\rho_2)\,\mathrm{J}_\nu(k_1\rho_1)\left\{\mathrm{H}_\nu'^{(2)}(k_2\rho_1)\,\mathrm{J}_\nu'(k_2\rho_2)-\mathrm{H}_\nu'^{(2)}(k_2\rho_2)\,\mathrm{J}_\nu'(k_2\rho_1)\right\}+ \frac{k_1k_2}{\mu_1\mu_2}\mathrm{J}_\nu'(k_1\rho_1)\,\mathrm{H}_\nu^{(2)}(k_3\rho_2)\left\{\mathrm{H}_\nu'^{(2)}(k_2\rho_2)\,\mathrm{J}_\nu(k_2\rho_1)-\mathrm{H}_\nu^{(2)}(k_2\rho_1)\,\mathrm{J}_\nu'(k_2\rho_2)\right\}+ \frac{k_1k_3}{\mu_1\mu_3}\mathrm{J}_\nu'(k_1\rho_1)\,\mathrm{H}_\nu'^{(2)}(k_3\rho_2)\left\{\mathrm{H}_\nu^{(2)}(k_2\rho_1)\,\mathrm{J}_\nu(k_2\rho_2)-\mathrm{H}_\nu^{(2)}(k_2\rho_2)\,\mathrm{J}_\nu(k_2\rho_1)\right\}+ \frac{k_2k_3}{\mu_2\mu_3}\mathrm{H}_\nu'^{(2)}(k_3\rho_2)\,\mathrm{J}_\nu(k_1\rho_1)\left\{\mathrm{H}_\nu^{(2)}(k_2\rho_2)\,\mathrm{J}_\nu'(k_2\rho_1)-\mathrm{H}_\nu'^{(2)}(k_2\rho_1)\,\mathrm{J}_\nu(k_2\rho_2)\right\}\right], \quad (43)$$

and

$$B(k_1,k_2,k_3,\rho_1,\rho_2,\rho_3) = \left[\frac{k_2^2}{\mu_2^2}\mathrm{J}_\nu(k_3\rho_2)\,\mathrm{J}_\nu(k_1\rho_1)\left\{\mathrm{H}_\nu'^{(2)}(k_2\rho_2)\,\mathrm{J}_\nu'(k_2\rho_1)-\mathrm{H}_\nu'^{(2)}(k_2\rho_1)\,\mathrm{J}_\nu'(k_2\rho_2)\right\}+ \frac{k_1k_2}{\mu_1\mu_2}\mathrm{J}_\nu'(k_1\rho_1)\,\mathrm{J}_\nu(k_3\rho_2)\left\{\mathrm{H}_\nu^{(2)}(k_2\rho_1)\,\mathrm{J}_\nu'(k_2\rho_2)-\mathrm{H}_\nu'^{(2)}(k_2\rho_2)\,\mathrm{J}_\nu(k_2\rho_1)\right\}+ \frac{k_1k_3}{\mu_1\mu_3}\mathrm{J}_\nu'(k_1\rho_1)\,\mathrm{J}_\nu'(k_3\rho_2)\left\{\mathrm{H}_\nu^{(2)}(k_2\rho_2)\,\mathrm{J}_\nu(k_2\rho_1)-\mathrm{H}_\nu^{(2)}(k_2\rho_1)\,\mathrm{J}_\nu(k_2\rho_2)\right\}+ \frac{k_2k_3}{\mu_2\mu_3}\mathrm{J}_\nu'(k_3\rho_2)\,\mathrm{J}_\nu(k_1\rho_1)\left\{\mathrm{H}_\nu'^{(2)}(k_2\rho_1)\,\mathrm{J}_\nu(k_2\rho_2)-\mathrm{H}_\nu^{(2)}(k_2\rho_2)\,\mathrm{J}_\nu'(k_2\rho_1)\right\}\right]. \quad (44)$$

Thus, analytical closed form representations are readily available for 2- and 3- layer capped wedge. Without resorting to numerical matrix inversion, these coefficients can be used directly for field calculation.

4. Numerical Simulations

Explicit forms for 2- and 3-layer capped wedge are utilized for numerical simulation of several wedge problems. To observe the influence of different parameters such as radius of the layer (ρ), relative permittivity (ε_r), relative permeability (μ_r), and loss tangent ($\tan\delta$) on the scattered electric field with plane wave excitation, numerical results are presented in Figures 2 through 9. The variation of the scattered field pattern is normalized as $|E_z| / |E_0|$. Analytical expressions for two different wedge angles and different layer properties are computed and compared to PEC-only case. The wedge angles of 10° and 30° are chosen to represent airplane wing geometries, but closed form expressions can be used for any wedge angle. Dielectric layer parameters are chosen from well-known materials.

First, permittivity values of 2-layer geometry with different loss tangents are studied. Magnitude of the electric field is presented in Fig. 2. More than 50 % reduction in magnitude is observed compared to PEC-only case. Small loss tangent did not make any considerable change in the electric field magnitude. Increased loss tangent values, of course, would increase the scattered field. Next, the same wedge shape with the same permittivity but different

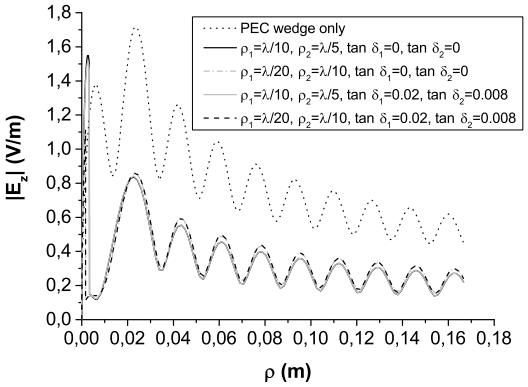

Fig. 2. Comparison of z components of electric field with respect to ρ. The parameters are $N = 2$, $\varepsilon_1 = 4.4$, $\varepsilon_2 = 2.2$, $\alpha = 30°$, $f = 9$ GHz and $\varphi = 180°$.

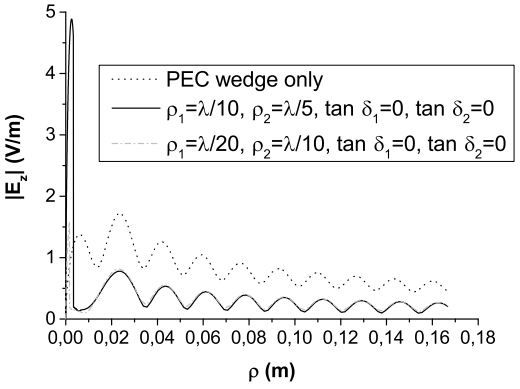

Fig. 3. Comparison of z components of electric field with respect to ρ. The parameters are $N = 2$, $\mu_1 = 7$, $\mu_2 = 4$, $\alpha = 30°$, $f = 9$ GHz and $\varphi = 180°$.

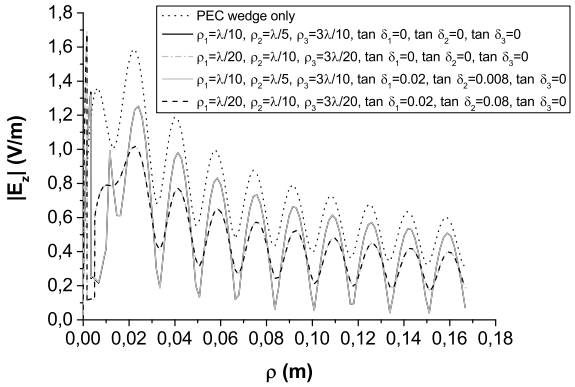

Fig. 4. Comparison of z components of electric field with respect to ρ. The parameters are $N = 3$, $\varepsilon_1 = 6$, $\varepsilon_2 = 4.4$, $\varepsilon_3 = 2.2$, $\alpha = 10°$, $f = 9$ GHz and $\varphi = 180°$.

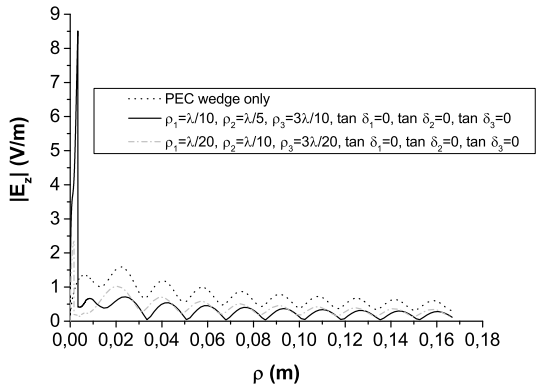

Fig. 5. Comparison of z components of electric field with respect to ρ. The parameters are $N = 3$, $\mu_1 = 11$, $\mu_2 = 7$, $\mu_3 = 4$, $\alpha = 10°$, $f = 9$ GHz and $\varphi = 180°$.

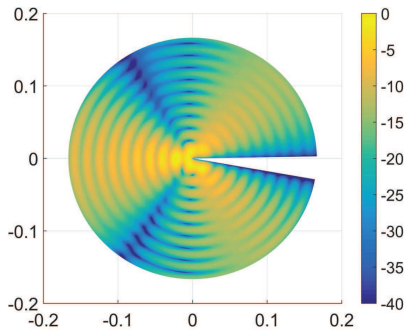

Fig. 6. Variation of $|\ E_Z\ |$(dBV/m) for standalone PEC wedge. The parameters are $\alpha = 10°$, $f = 9$ GHz and $\varphi_0 = 180°$.

permeability values are presented in Fig. 3. Again, the field magnitude was reduced more than half with this configuration. The thickness of the layers did not substantially influence the magnitude. The spike in field magnitude near the tip of the wedge was larger than PEC-only case as field localized in this asymptotic region was enhanced due to permeability of the layer.

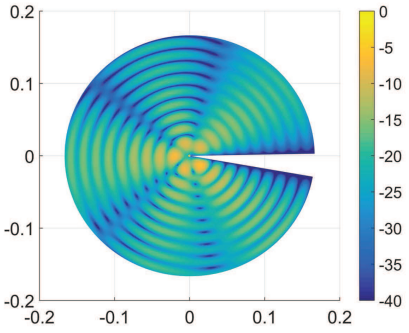

Fig. 7. Variation of $|\ E_Z\ |$(dBV/m). The parameters are $N = 2$, $\rho_1 = \lambda : 20$, $\rho_2 = \lambda : 10$, $\tan\delta_1 = 0$, $\tan\delta_2 = 0$, $\alpha = 10°$, $f = 9$ GHz and $\varphi_0 = 180°$.

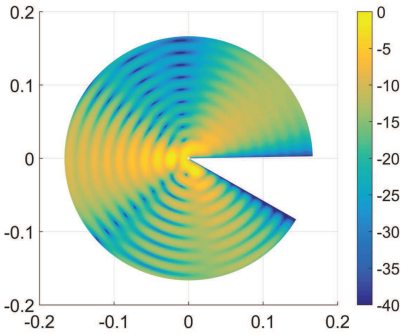

Fig. 8. Variation of $|\ E_Z\ |$(dBV/m) for standalone PEC wedge. The parameters are $\alpha = 30°$, $f = 9$ GHz and $\varphi_0 = 180°$.

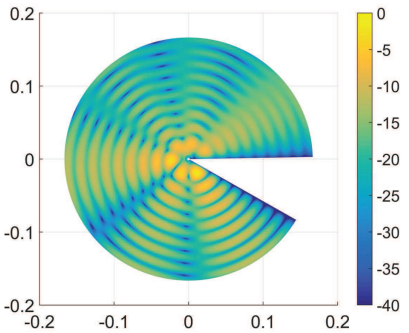

Fig. 9. Variation of $|\ E_Z\ |$(dBV/m). The parameters are $N = 3$, $\rho_1 = \lambda : 20$, $\rho_2 = \lambda : 10$, $\rho_3 = 3\lambda : 20$, $\tan\delta_1 = 0$, $\tan\delta_2 = 0$, $\tan\delta_3 = 0$, $\alpha = 30°$, $f = 9$ GHz and $\varphi_0 = 180°$.

Similar analysis was carried out for narrower wedge angle of 10° in Figures 4 and 5. It is observed that the effects of dielectric layers were slightly less than those of 30° wedge angle as expected. As the wedge angle gets smaller, incident plane encounters less cross sectional area of the wedge, which in turn, leads to lowered electric field magnitude in

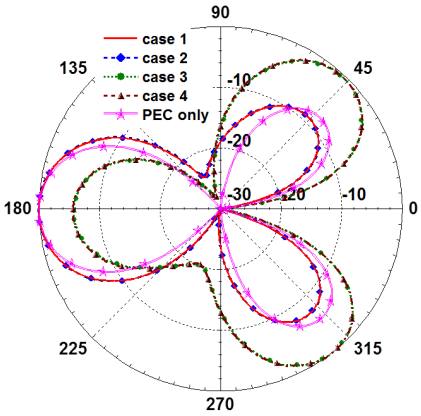

Fig. 10. Modified RCS pattern (dB) for $\alpha = 10°$, $\varphi_0 = 180°$, $\varepsilon_1 = 4.4$ and $\varepsilon_2 = 2.2$, for Cases 1-4 and PEC-only case. Case 1: N = 2, $\rho_1 = \lambda : 10$, $\rho_2 = \lambda : 5$, $\rho_0 = 3\lambda : 5$, $\tan\delta_1 = 0$, $\tan\delta_2 = 0$, Case 2: $N = 2$, $\rho_1 = \lambda : 10$, $\rho_2 = \lambda : 5$, $\rho_0 = 3\lambda : 5$, $\tan\delta_1 = 0.02$, $\tan\delta_2 = 0.008$, Case 3: $N = 2$, $\rho_1 = \lambda : 5$, $\rho_2 = 2\lambda : 5$, $\rho_0 = 6\lambda : 5$, $\tan\delta_1 = 0$, $\tan\delta_2 = 0$, Case 4: $N = 2$, $\rho_1 = \lambda : 5$, $\rho_2 = 2\lambda : 5$, $\rho_0 = 6\lambda : 5$, $\tan\delta_1 = 0.02$, $\tan\delta_2 = 0.008$.

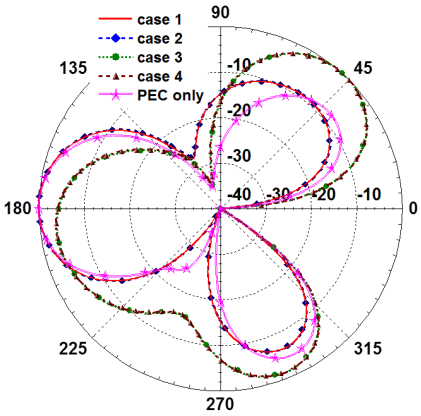

Fig. 11. Modified RCS pattern (dB) for $\alpha = 30°$, $\varphi_0 = 180°$, $\varepsilon_1 = 4.4$ and $\varepsilon_2 = 2.2$, for Cases 1-4 and PEC-only case. Case 1: N = 2, $\rho_1 = \lambda : 10$, $\rho_2 = \lambda : 5$, $\rho_0 = 3\lambda : 5$, $\tan\delta_1 = 0$, $\tan\delta_2 = 0$, Case 2: $N = 2$, $\rho_1 = \lambda : 10$, $\rho_2 = \lambda : 5$, $\rho_0 = 3\lambda : 5$, $\tan\delta_1 = 0.02$, $\tan\delta_2 = 0.008$, Case 3: $N = 2$, $\rho_1 = \lambda : 5$, $\rho_2 = 2\lambda : 5$, $\rho_0 = 6\lambda : 5$, $\tan\delta_1 = 0$, $\tan\delta_2 = 0$, Case 4: $N = 2$, $\rho_1 = \lambda : 5$, $\rho_2 = 2\lambda : 5$, $\rho_0 = 6\lambda : 5$, $\tan\delta_1 = 0.02$, $\tan\delta_2 = 0.008$.

PEC-only case. Lossless dielectric layers were more successful in reducing the scattered electric field.Variation of electric field magnitude at z = 0 plane was also studied for both wedge angles. In Figures 6 and 7, PEC-only case and permittivity varied case were shown, respectively. Reduction in electric field magnitude was greater than 3 dB in almost every direction. PEC-only case for 30° wedge angle is displayed in Fig. 8 and 3-layer case with different permittivity values are shown in Fig. 9.

Far-field analysis of the electric field can be expressed as

$$\sigma' = \lim_{\rho\to\infty} 2\pi\rho \frac{|E_{\text{tot}}|^2}{|E_{\text{inc}}|^2}$$

where σ' denotes modified RCS as total electric field instead of scattered electric field is considered. For 10° and 30° wedge angles, four different cases are compared to PEC only case in Figures 10 and 11, respectively. The incident electric field is assumed from 180° direction to the wedge. It is observed that for monostatic radar applications, Cases 3 and 4 provide 5.8 and 5.7 dB reduction relative to PEC-only case on incident wave direction, whereas Cases 1 and 2 provide almost no reduction but about 1 dB reduction at +/-20° off of incident direction. On opposite side of the incident direction, layered wedge has more RCS compared to PEC-only case as expected. Since Cases 1, 3 and Cases 2, 4 differ only for layer thicknesses with other parameters being equal, layer thicknesses play a critical role in achieving RCS reduction.

5. Conclusions

Layered capped wedge with various thicknesses and dielectric loss values have been studied for electric field magnitude in longitudinal direction. Explicit expressions for 2- and 3-layer geometries are derived rigorously. It is observed that for certain values of cap radii and loss factors, more than 3 dB reduction in scattered electric field is possible with 2- and 3-layer cap geometries in the near field. Similar analysis is also carried out for modified RCS to compare far-field effects of capped wedge and it is observed that almost 6 dB reduction is possible for certain combination of layer thicknesses. The dielectric layer thicknesses were kept small to enable coating on the PEC surface at the target frequency of 9 GHz. This particular frequency is chosen at X-band where most military radars operate. It is shown that with simple dielectic coating on wing-like airplane structures radar cross section can be reduced by more than half compared to PEC-only case.

Acknowledgments

This work was supported by TÜBİTAK (The Scientific and Technological Research Council of TURKEY) under BİDEB postdoctoral scholarship program.

References

[1] MENTZER, J. R. *Scattering and Diffraction of Radio Waves*. 1st ed. New York, NY (USA): Pergamon Press, 1955.

[2] FELSEN, L. B., MARCUVITZ, N. *Radiation and Scattering of Waves*. Piscataway, NJ (USA): IEEE Press, 1994. ISBN: 978-0780310889

[3] HARRINGTON, R. F. *Time-Harmonic Electromagnetics Field*. 1st ed. New York, NY (USA): McGraw & Hill, 1961.

[4] BOWMAN, J. J., SENIOR, T. B. A., USLENGHI, P. L. E. *Electromagnetic and Acoustic Scattering by Simple Shapes*. New York, NY (USA): Hemisphere Publishing, 1987.

[5] REDADAA, S., BOUALLEG, A., MERABTINE, N., et al. Radar cross section study from wave scattering structures. *Semiconductor Physics, Quantum Electronics & Optoelectronics*, 2006, vol. 9, no. 4, p. 71–76.

[6] LEWIN, L., SREENIVASIAH, I. *Diffraction by a Dielectric Wedge, Technology Report*. 191 pages.

[7] MALIUZHINETS, G. D. Excitation, reflection, and emission of surface waves from a wedge with given face impedances. *Soviet Physics Doklady*, 1958, vol. 3, p. 752–755.

[8] FELSEN, L. B. Electromagnetic properties of wedge and cone surfaces with a linearly varying surface impedance. *IRE Transactions on Antennas and Propagation*, Dec. 1959, vol. 7, p. 231–243. DOI: 10.1109/TAP.1959.1144752

[9] ISENLIK, T., YEGIN, K. Paraxial fields of a wedge with anisotropic impedance and perfect electric conductor faces excited by a dipole. *Electromagnetics*, 2010, vol. p. 30, no. 7, 589-608. DOI: 10.1080/02726343.2010.513932

[10] ISENLIK, T., YEGIN, K. Derivations of Green's functions for paraxial fields of a wedge with particular anisotropic impedance faces. *Electromagnetics*, 2013, vol. 33, no. 5, p. 392–412. DOI: 10.1080/02726343.2013.792722

[11] ENGHETA, N., MURPHY, W. D., ROKHLIN, V., et al. The fast multipole method (FMM) for electromagnetic scattering problems. *IEEE Transactions on Antennas and Propagation*, 1992, vol. 40, no. 6, p. 634–641. DOI: 10.1109/8.144597

[12] ERGUL, O., GUREL, L. *The Multilevel Fast Multipole Algorithm (MLFMA) for Solving Large-Scale Computational Electromagnetics Problems*. Piscateway, NJ (USA): Wiley-IEEE Press, 2014. ISBN: 978-1-119-97741-4

About the Authors . . .

Hulya OZTURK was born in 1984 in İstanbul, Turkey. She received her M.Sc. and Ph.D. degree in mathematics from Gebze Technical University, Kocaeli, Turkey, in 2010 and 2015, respectively. Her research interests are in electromagnetic and acoustic wave scattering and propagation.

Korkut YEGIN received the B.Sc. degree in electrical and electronics engineering from Middle East Technical University, Ankara, Turkey, in 1992, the M.Sc. degree in electrical and computer engineering, the M.Sc. degree in plasma physics, and the Ph.D. degree in electrical and computer engineering from Clemson University, Clemson, SC, USA, in 1996, 1998 and 1999, respectively. He is a professor at Ege University Electrical and Electronics Engineering , İzmir, Turkey. His research interests include electromagnetic scattering, VSAT antennas, and UWB radar.